Application of Dang Van criterion to rolling contact fatigue in wind turbine roller bearings

Michele Cerullo

Department of Mechanical Engineering ,Technical University of Denmark, Lyngby 2100, Denmark
mcer@mek.dtu.dk

Abstract A 2-D plane strain finite element simulation of rolling contact in wind turbine roller bearings is used to study very high cycle fatigue (VHCF). Focus is on fatigue in the inner ring, where the effect of residual stresses and hardness variation along the depth are accounted for. The purpose here is to ensure that VHCF failure does not initiate. For the purpose the Dang Van multiaxial fatigue criterion is applied, simulating the contact on the bearing raceway by substituting the roller with the Hertzian static pressure distribution. Contact without friction is assumed here and the material used for the simulation is taken to be an AISI 52100 bearing steel. Both an initially stress free bearing and different residual stress distributions are considered. An assumed residual stress distribution, equilibrated by an elastic step calculation, is subsequently subjected to the stresses caused by the contact with the roller. The effect of variable hardness along the depth is also studied, relating its values to the fatigue limit parameters for the material and it is found that its distribution can have a significant influence on the probability of failure for bearings subjected to VHCF loading.

Keywords High Cycle Fatigue, Wind turbine, Dang Van

1. Introduction

It has been seen [1,2] that one of the important reasons of corrective maintenance for a wind turbine is a failure due to rolling contact fatigue (RCF) in one of the bearings in the gear box [3]. Therefore, the interest on the reliability of gearboxes grew over the last years [4,5]. Though failure rates in electrical systems and other subassemblies in a wind turbine are in fact higher, or at least comparable with faults in the gearbox, recent studies [6–8] show that the downtime, in terms of hours lost per failure, is much higher for latter ones. This, rather than the failure rate, is therefore one of the main reasons for the industry's focus on these subsystems.
In the gearbox, the bearings used are mostly roller bearings, due to the high loads involved. Even if the lubricant is kept clean and the bearing is properly lubricated, roller bearings sometimes experience rolling contact fatigue that appears as a crack starting below the surface of the inner race [9]. Once nucleated, this crack quickly propagates to the surface, resulting in particles of material flaking and leading to the failure of the bearing. Roller bearings for wind turbine applications operate in the fully elastic range and are subjected to a very high number of load cycles, with an expected life of 20 years [10]. However, practical experience show a high life scatter in these machinery elements, with failures that sometimes occur after a few years. The failure of these elements is thought to be due mainly to inhomogeneities and nonmetallic inclusions, that act as sites for crack nucleation under rolling contact fatigue. The cracks usually nucleate around inclusions, where the material experiences high stress concentration and typical butterfly defects are observed.
The modelling in the present paper is focused on ensuring that the cyclic stress fields stay within limits so that very high cycle fatigue damage does not initiate. Several multiaxial fatigue models have been developed [11–15], and some of them have been applied to RCF problems. The Dang Van criterion [16] and its further modifications has been widely used, over the last decades, in automotive industry [17] and in rolling contact problems as railwails and bearings [18,19]. It seems that the Dang Van criterion is not sufficiently conservative for negative values of the hydrostatic stress, therefore a modified version has been recently proposed [20], predicting a less sensitive behavior with respect to this stress component. This paper also includes a study of the overall effect

of pre-existing residual stresses in the material, resulting from hardening process. Using the Dang Van criterion, different residual stresses and hardening distributions are studied, and results are compared.

2. Problem formulation

Part of the initial geometry of the inner ring of the roller bearing is illustrated in Fig. 1. The inner ring and the shaft have been considered as one body of external radius $R=R_s+t_k$, where R_s is the shaft radius and t_k is the thickness of the inner ring. This assumption is equivalent to neglecting contact stresses related to the mounting and any local stress concentrations at the interface between ring and the shaft.

In order to reduce the computational time, only an angular sector of the solid, with angular width $\alpha=10°$, has been modeled. Far away from the surface, the region analyzed is terminated by a circular arc boundary with radius r. Along the edges, the solid is free to slide in the radial direction, being constrained in the direction perpendicular to the edges. A cartesian coordinate system Oxyz is used, with the origin O in the center of curvature of R, the axis z pointing out of the paper, and the axes x and y, respectively, horizontally and vertically aligned. As a 2-D model is studied, no edge effects in the direction perpendicular to the plane of the model are accounted for. The pressure acting on the raceway and resulting from the contact with the roller, is evaluated according to classical Hertzian theory, and is considered identical in any plane parallel to xy:

$$p(x,y)=p_0\,[1-(\frac{x-x_p}{a})^2-(\frac{y-y_p}{a})^2]^{0.5} \tag{1}$$

In Eq.(1), p_0 is the maximum value of the pressure, x_p and y_p the coordinates of the center of the contact area, a the semi-width of the contact area under the roller and x and y the coordinates of a generic point on the surface in the contact area. The value of p_0 is related to the force acting on the roller by the relation

$$p_0=\sqrt{\frac{q}{\pi}\frac{\Delta}{\rho}} \tag{2}$$

where Δ is function of the Young moduli E_i and Poisson ratios ν_i of the roller and the inner race, here assumed of the same material. The constant ρ is a pure function of the curvature radii and q=F/L is the force per unit length acting on the roller.

A bearing with the inner ring thickness t_k=19 mm, mounted on a shaft of R_s=200 mm, has been used in the simulations. Furthermore values of 70 mm and 20 mm, respectively, are assumed for the length and the radius of the roller. A load of 37 KN is considered pushing the roller against the inner race, resulting in a static Hertzian maximum pressure p_0~1 GPa. The contact is assumed continuous without any vibrations effects. No friction or sliding are here accounted for.

The pressure distribution, that simulates the contact, is assumed to move along the surface, in a region where the mesh is uniform. Far away from the zone affected by the contact stresses, instead, the elements are stretched, both in the radial and in the tangential direction, close to the edges. The material is considered isotropic, with Young modulus E=210 GPa and Poisson ratio ν=0.3.

In terms of the displacement components u_i on the reference base vectors the strain tensor is given by

$$\varepsilon_{i,j}=\frac{1}{2}(u_{i,j}+u_{j,i}) \tag{3}$$

where $()_{,j}$ denotes partial differentiation. The equilibrium equations, written in terms of the stress tensor σ_{ij} and the strain tensor ε_{ij}, are obtained by the use of the principle of virtual work:

$$\int_V \sigma_{ij}\delta\varepsilon_{ij}\,dV=\int_S T_i u_i\,dS \tag{4}$$

where V and S are the volume and surface of the region analyzed, and T_i are the specified surface tractions.

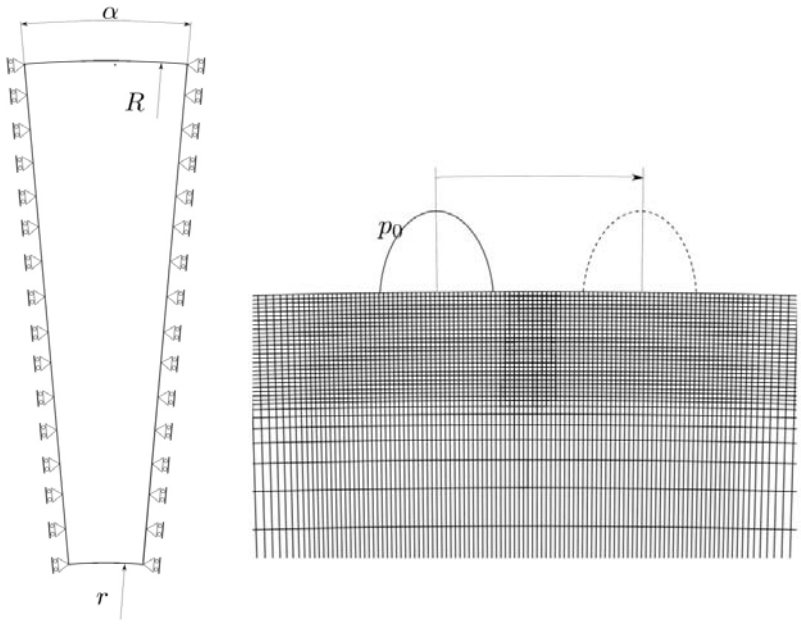

(a) (b)

Figure 1. (a) Geometry used to model the problem: r=100mm, R_s=200mm, t_k=19 mm, α=10°. (b) A detail of the mesh used.

2.1 The Dang Van criterion

A brief introduction to the basis of the fatigue criterion used will be given (see further details in [16]). The Dang Van criterion is a stress based multiaxial fatigue criterion. It relates the variation of the stress state in a material point to a critical parameter, that should not be reached:

$$f[\sigma_{ij}(t)] \leq \lambda \tag{5}$$

The critical value λ is usually function of the fatigue limits in pure torsion, τ_w, and the fatigue limit in pure bending, σ_w, and its choice is essential in a multiaxial criterion since it establishes which is the most important stress component that is assumed to have influence on the failure. The Dang Van criterion, in particular, can be formulated as:

$$\tau_{max}(t)+\alpha_{DV}\sigma_H(t) \leq \tau_w \tag{6}$$

where

$$\alpha_{DV}= 3\left(\frac{\tau_w}{\sigma_w}-\frac{1}{2}\right) \tag{7}$$

is a constant that depends on the material fatigue limits previously mentioned, $\sigma_H(t)$ is the instantaneous hydrostatic component of the stress tensor and $\tau_{max}(t)$ is the instantaneous value of the Tresca-like shear stress

$$\tau_{max}(t)= \frac{\widehat{\sigma_I}(t)-\widehat{\sigma_{III}}(t)}{2} \tag{8}$$

The stress deviator is obtained by the usual definition:

$$s_{ij}(t)=\sigma_{ij}(t)- \delta_{ij}\sigma_H(t) \tag{9}$$

Then a constant tensor, s_{ij}^m, is calculated by solving the minmax problem

$$s_{ij}^{m}=\min_{s_{ij}^{*}} \max_t [(s_{ij}(t)-s_{ij}^{*})(s_{ij}(t)-s_{ij}^{*})] \quad (10)$$

and the shifted deviator tensor is defined as

$$\widehat{s_{ij}}(t)=\sigma_{ij}(t)- s_{ij}^{m} \quad (11)$$

The principal values of the shifted tensor appear in Eq. (8).
The problem in Eq. (10) is solved iteratively using a move limit approach :

$$s_{ij}^{m}=\min_{s_{ij}^{*}} \max_t [(s_{ij}(t)-s_{ij}^{*})(s_{ij}(t)-s_{ij}^{*})] =\min_{s_{ij}^{*}} [\max_t \Phi] \quad (12)$$

with

$$\Phi=\Phi (t, s_{ij}(t), s_{ij}^{*}) \quad (13)$$

Choosing an arbitrarily starting value for s_{ij}^{*}, for example the average deviatoric stress tensor in the stress history for that material point, then for every iteration we identify the maximum value of Φ. Let t_m be the time step at which $\max \Phi$ happen, then the value of s_{ij}^{*} is updated

$$s_{ij}^{*}=s_{ij}^{*}+ ds_{ij}^{*} \quad (14)$$

with

$$ds_{ij}^{*}=\gamma (s_{ij}(t_m)-s_{ij}^{*}) \quad (15)$$

which can be interpreted as a modified steepest descend method. If at one step Φ increases, γ is reduced to 0.25 γ. The iteration is stopped if the norm of the difference between s_{ij}^{*} at the current iteration step k and at the previous step falls into a tolerance range:

$$\left\| s_{ij}^{*}]_k - s_{ij}^{*}]_{k-1} \right\| \le \varepsilon_{toll} \quad (16)$$

Although a superimposed hydrostatic tension has an effect on the fatigue life in normal cyclic loading [21], several studies [11] have shown that a superimposed mean static torsion has no effect on the fatigue limit of metals subjected to cyclic torsion. The independency of the mean shear stress is correctly predicted through the minimization process in Eq. (10), see also [20]. The Dang Van criterion could also be used with $\tau_{max}(t)$ representing the maximum shear stress at every point of the stress history. Then, one would not account for the experimental observation that in cyclic torsion fatigue failure is independent of the mean shear stress, and this would usually result in lower permitted stress levels.
The Dang Van proposal is equivalent to request, in the $\sigma_H(t)$ - $\tau_{max}(t)$ plane, that all the representative points of the stress state, fall below the line intersecting the $\tau_{max}(t)$ axis in τ_w with a negative slope of α: if all of the points fulfill this requirement, the criterion predicts a safe life for the component (see Fig. 2).
The original Dang Van safe locus predicts a detrimental effect of tensile hydrostatic stress while an over-optimistic positive effect is expected from compressive values. The negative effect of tensile mean stress is well known in literature from classic Haigh diagrams, that also show a flat response for negative stress ratios [22, 23]. For this reason it is not too conservative to choose a different safe locus in the Dang Van plane to be in agreement with this response, for example a bilinear limit curve, as proposed recently in [20]. The safe locus could be therefore identified in two segments, one with a null slope and the other one with a negative slope equal to α (Fig. 2). For $\sigma_H(t) \ge \sigma_A$ the safe region is identical to the original Dang Van region, while for smaller values of σ_A, the cut-off with the flat curve replaces the Dang Van limit curve by a curve more on the safe side. Values of $\sigma_A = \sigma_w/3$ and of $\tau_A = \sigma_w/2$ have been proposed in [20], on the basis of experimental results obtained on high-strength steel smooth specimens. However, it is possible to choose a different set of values for (σ_A, τ_A), though here the same choice has been made. If the ratio of the fatigue limits, σ_w/τ_w, was equal to 0.5, the value α_{DV} in Eq. (6) would be zero, which is far from reality, as steels usually

show ratios between 0.57 and 0.8 [21]. Anyway, it is always possible to assume different values of σ_A, more or less conservative than the cut off shown in Fig 2.
In the following sections, both the original safe locus and a new one with the mentioned cut-off will be used, and results will be compared. For τ_w a value of 360 MPa has been imposed [24] and a ratio $\sigma_w/\tau_w=\sqrt{3}$. With this assumption the value of the constant α_{DV} used in the calculations is approximately 0.23205.

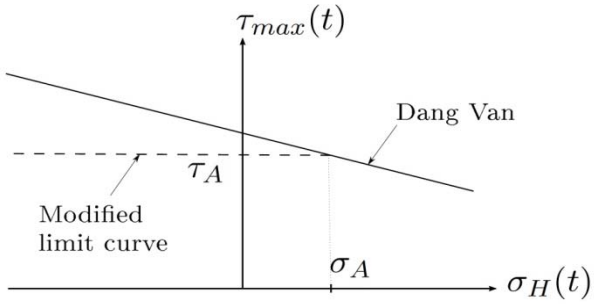

Figure 2. The Dang Van safe locus: the dashed line represents the alternative limit curve, for $\sigma_H(t)<\sigma_A$, here assumed equal to $\sigma_w/3$, as proposed in [20].

For a material point subjected, at time t, to $\sigma_H(t)$ and $\tau_{max}(t)$, the ratio between $\tau_{max}(t)$ and the corresponding limit value for that $\sigma_H(t)$ is here used to define the damage factor n(t). Points on the limit curve, then, result in a unit damage factor; points inside the safe region have damage factor smaller than one. As previously mentioned, two different safe loci are here used: one with a linear limit curve and another one with a bilinear limit curve. Consequently, a damage factor is here defined as

$$n(t)= \frac{\tau_{max}(t)}{\tau_w-\alpha_{DV}\,\sigma_H(t)} \tag{17}$$

if referred to the original Dang Van's safety region or

$$n(t)=\begin{cases} \dfrac{\tau_{max}(t)}{\tau_w-\alpha_{DV}\,\sigma_H(t)} & \text{if } \&\sigma_H>\sigma_A \\ \dfrac{\tau_{max}(t)}{\tau_A} & \&\text{if } \sigma_H\le\sigma_A \end{cases} \tag{18}$$

when the bilinear limit curve is used. As mentioned above, σ_A and τ_A are chosen equal to $\sigma_w/3$ and $\sigma_w/2$, respectively.

3. Results and discussion

The Dang Van criterion has been applied to the rolling contact problem and for the geometry described in section 2. The load history has been divided in an adequate number of steps and, for each time step, the value of the damage factor n(t) has been calculated, both with the original Dang Van limit curve and with the modified one. The maximum value in time

$$n= \max_t n(t) \tag{19}$$

is then chosen, as representative for that material point. If this $n<1$, the prediction is that initiation of fatigue failure will not occur in the material point. The representative points corresponding to the max value of the damage factor are plotted, in Fig. 3, in the Dang Van region, for all the integration points in the region analyzed.
In Fig. 4 the maximum values of this factor n are plotted against the distance from the surface. Both safe regions, as described before, are used. As we can see, n reaches the highest value in a sub-surface region, about 0.20 mm below the surface : this is consistent with literature, where a lot of sub-surface initiated failures in bearings for windmill applications are reported.

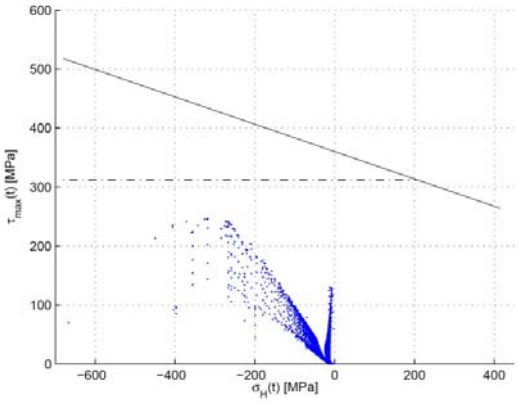

Figure 3. The Dang Van criterion: in order that the failure does not occur, all the representative points should be inside the safe region delimited by the limit curves. In this figure, and for the problem considered, only the representative points corresponding to max value of the damage factor are plotted for all the integration points in the region analyzed.

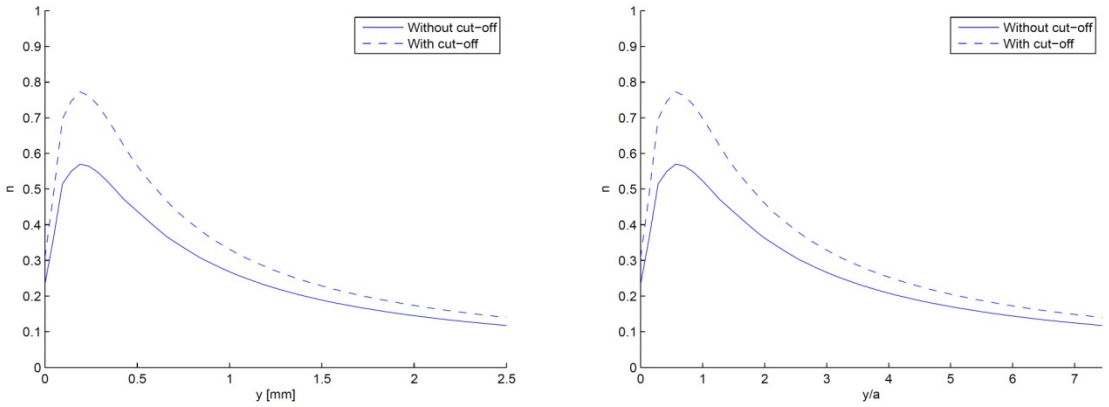

(a) (b)

Figure 4. Damage factor versus distance from surface (a) and versus distance from surface non dimensionalized by the half contact width (b).

3.1 Hardness variation

The relationships between fatigue strength, the hardness and the ultimate tensile strength are used, in this section, to study the influence of the hardness variation in the inner ring.
Since fatigue crack initiation is mainly caused by slip within grains, the yield stress, in the past, has been thought to have the strongest correlation with the fatigue limit. However Murakami [25] has found better correlations between tensile strength, hardness and fatigue limits.
In order to correlate the hardness to the fatigue limit, τ_w, this limit has first been related to σ_{UTS} through an approximate expression proposed in [26] for low-alloy steels:

$$\tau_w=\sigma_w/\sqrt{3}\approx 0.274\ \sigma_{UTS} \tag{20}$$

Denoting the Brinell hardness by HB and using an approximate relationship found in [27]

$$\sigma_{UTS}=0.0012\ HB^2+3.3\ HB \tag{21}$$

an approximate final relation between τ_w and HB can be written as

$$\tau_w=0.274\ (0.0012\ HB^2+3.3\ HB) \tag{22}$$

In the following we assume that the fatigue limit τ_w is given by the Eq. (22). If another expression $\tau_w(HB)$ applies for a material, this will not in principle change the procedure. In fact, all we need is

the value of τ_w in each material point of the solid analyzed.
Different hardness distributions along the depth have been studied here. Thus the value of τ_w corresponding to the value of the hardness at that depth has been imposed in the material for each Gauss integration point.
The different hardness distributions imposed in the subsurface region of inner ring and the correspondent τ_w distributions are shown in Fig. 5 (a)–(d). At distances greater than 1 mm from the surface, HB, for distributions (a) and (b), are taken to be constant, at a value such that the related fatigue limit, $\tau_w=\tau_w(HB)$, is approximately 360 MPa. This assumption is equivalent to considering how the effect of a surface hardening process would benefit the fatigue response of the bearing. Results show that the values of the damage factor n and the depth at which the maximum n is reached, are strongly dependent on the particular distribution of hardness imposed (Fig. 6).

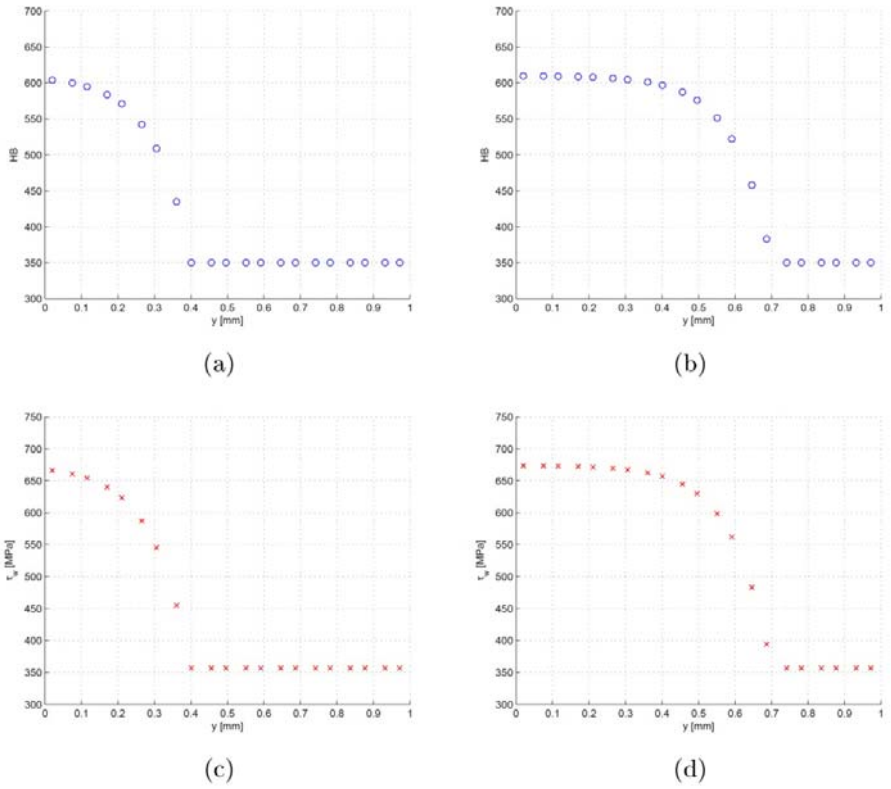

Figure 5. Hardness distributions ((a)-(b)) and correspondent values of τ_w ((c)-(d)) in the first millimeter of depth .

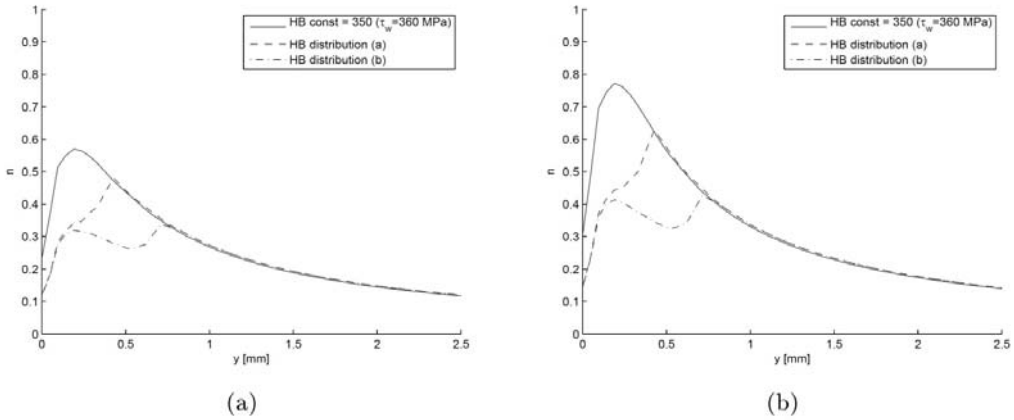

Figure 6. Damage factor versus distance from surface. In (a) the original Dang Vang safe locus has been used, while in (b) the bilinear limit curve, as described in section 2.1. The different distributions are referred to Fig. 5.

For all the cases analyzed, the peak of the n-curve shifts away from the surface of the inner ring and, for cases shown in Figs. 5a and 5b, the peak values of n are smaller than the correspondent peaks for a material with uniform hardness. In other words, the rings with extra surface hardening have higher safety against fatigue failure.

3.2 Residual stresses

In order to analyze the influence of pre-existing stresses in the bearing, two different residual stress distributions have been considered. The bearing with the assumed residual stress distribution, equilibrated by an elastic step calculation, is subsequently subjected to the stresses caused by the contact with the roller. The results obtained with the Dang Van criterion are then compared with the results obtained in the bearing free of residual stresses.

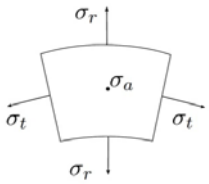

Figure 7. Convention used for the principal stresses in the polar coordinate system.

In Fig. 7 the convention used to name the residual stresses is clarified, while, in Figs. 8a and 8b, the residual stress distributions, in terms of principal stresses, are plotted versus the distance from the surface. Far away from the surface, the residual stresses are assumed to be constant and near zero.
The results for the two different safe loci (Fig. 2) are shown in Fig. 9. The pre-existing stress states in the inner ring, in the case of the modified safe locus, have little effect, neither positive nor negative (Fig. 9a). The residual stresses, in fact, result in a simple shift along the σ_H axis in the Dang Van region (Fig. 2) but this does not change the distance from the limit curve since all the most critical material points are subjected to values of σ_H smaller than σ_A and therefore they are in the region where the limit value for τ_{max} is constant and equal to τ_A. If the original limit curve is used, instead, the residual stress distribution (a) from Fig. 8 results in a reduction of the maximum damage factor for the compressive residual stresses, but an increase of the maximum damage factor for tensile residual stresses (Fig. 9b).

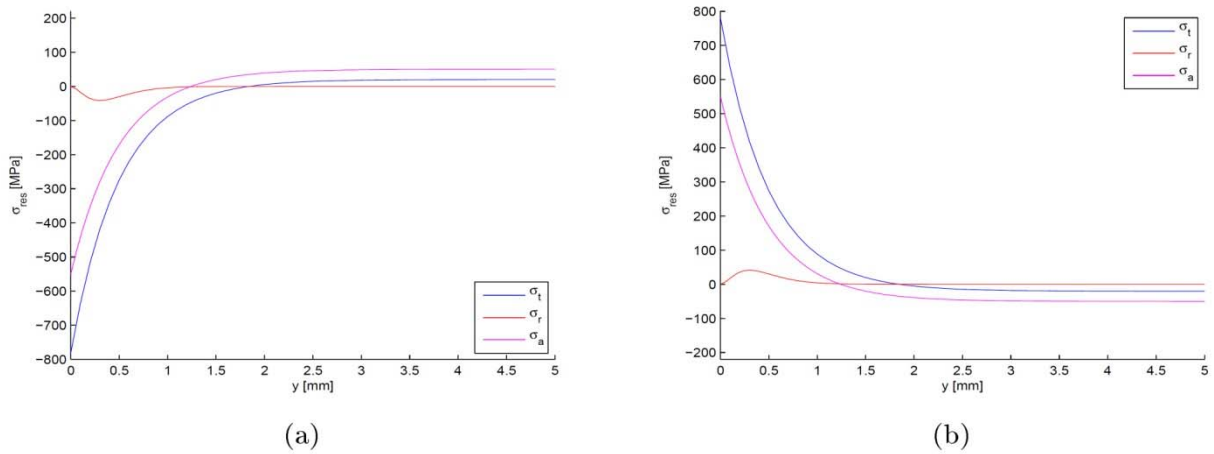

Figure 8. Residual stresses assumed in terms of principal stresses. Distribution (b) is obtained by multiplying (a) by -1.

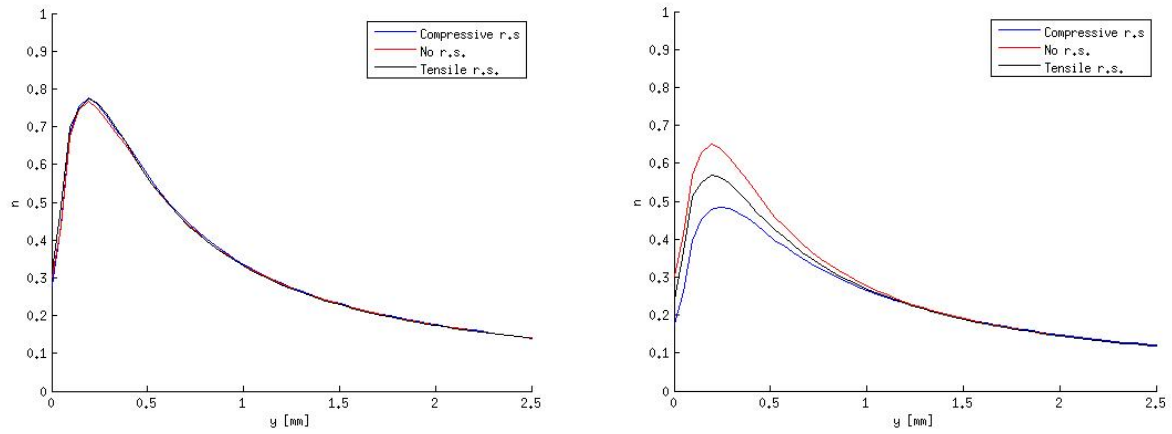

(a) (b)

Figure 9. Damage factor versus distance from surface for bilinear (a) and original limit curve (b).

4. Conclusions

The Dang Van criterion has been applied to a roller bearing for windmill applications and the influence of hardness variations and different residual stresses has been studied. Results have shown that, according to the Dang Van criterion, the highest damage factor is reached below the surface, regardless the safe locus used. This suggests that failure is most likely to initiate in the material a little below the surface, which is consistent with literature that reports subsurface failures of roller bearings for wind turbine applications.

The effect of increased hardness, in a thin layer close to the surface, has also been studied, relating the hardness to the fatigue strength of the material. The particular hardness distribution induced is seen to be important in evaluating the safety against fatigue for the bearing. Assuming that a higher fatigue strength corresponds to a higher Brinell hardness, the results indicate that a hardening surface treatment will be beneficial in terms of fatigue damage. However, surface hardening is not really possible for AISI 52100 bearing steel, though some recent work [28] seems to indicate an improvement of fatigue strength, for these steels, by induction heating and repeated quenching. It may be noted also that some steels show a maximum for the curve $\tau_w(\mathrm{HB})$, which would limit the applicability of Eq. (22). In fact, Eq.(22) is valid only for smaller values of hardness.

Bearings with different residual stress distributions have also been studied and calculations carried out show, for the Dang Van criterion, a positive effect of compressive residual stresses in the subsurface region according to the original safe locus. No influence of residual stresses has been found with the use of the modified safe locus and for the load case analyzed.

Acknowledgements

The author would like to thank Prof. Viggo Tvergaard and Associate Prof. Peder Kilt, Technical University of Denmark, for ideas, discussions and comments. This work is supported by the Danish Council for Strategic Research, in the DSF center REWIND.

References

[1] H. Arabian-Hoseynabadi, H. Oraee, P.J. Tavner, Failure Modes and Effects Analysis (FMEA) for wind turbines. Electrical Power and Energy Systems , 32 (2010) 817–824.

[2] Y. Amirat, M.E.H. Benbouzid, E. Al-Ahmar, B. Bensaker, S. Turri, Brief status on condition monitoring and fault diagnosis in wind energy conversion systems. Renew Sust Energ Rev, 13 (2009) 2629–2636.

[3] P.J. Blau, L.R. Walker, H. Xu, R.J. Parten, J. Qu, T. Geer, Wear analysis of wind turbine gearbox bearings - Final Report. Oak Ridge National Laboratory 2010.

[4] K. Smolders, Y. Feng, H. Long, P. Tavner Reliability Analysis and Prediction of Wind Turbine

Gearboxes. European Wind Energy Conference–EWEC 2010.
[5] C.Fernandes, R. C. Martins, Jorge H. O. Seabra, Friction torque of cylindrical roller thrust bearings lubricated with wind turbine gear oils. Tribology International (2012) (article in press).
[6] F. Spinato, P. J. Tavner, G. J. W. van Bussel, E. Koutoulakos, Reliability of Different Wind Turbine Concepts with Relevance to Offshore Application. European Wind Energy Conference 2008.
[7] F. Spinato, P. J. Tavner, G. J. W. van Bussel, E. Koutoulakos, Reliability of wind turbine subassemblies. IET Renewable Power Generation, 3 (2009) Issue 4, 387–401.
[8] Ma yang, He Chengbing, Feng Xinxin, Institutions Function and Failure Statistic and Analysis of Wind Turbine. Physics Procedia, 24 (2012), 25–30.
[9] F. Sadeghi, B. Jalalahmadi, T. S. Slack, N. Raje, N. K. Arakere, A Review of Rolling Contact Fatigue. Journal of Tribology, 131 (2009), Issue 4, 041403–1.
[10] A. Ragheb, M. Ragheb, Wind turbine gearboxes technologies. Proceedings of the 1st International Nuclear and Reneawble Energy Conference - INREC 2010.
[11] G. Sines, Behaviour of metals under complex static and alternating stresses, in: Metal Fatigue (eds. G. Sines and J.L. Waisman), McGraw-Hill, New York, 1959, pp. 145–169.
[12] W. N. Findley, Trans. ASME Ser B 81 (1959), 301.
[13] T. Matake, Bull. JSME 20 (1977), 257.
[14] D. L. McDiarmid, Fatigue Fract. Engng Mater. Struct. 17 (1994), 1475.
[15] I. V. Papadopoulos, Fatigue polycyclique des métaux: une nouvelle approche. Ph.d Thesis, spécialité: Mécanique, Ecole des Ponts et Chaussées, France, 1987.
[16] K. Dang Van, Sur la résistance à la fatigue des métaux. Sciences Technique Armement 47 (1973), 3.
[17] A.-S. Beranger, J.-V. Berard and J.-F. Vittori, A fatigue life assessment methodology for automotive components, in Fatigue Design of Components, in: ESIS Publication, 22, G. Marquis and J. Solind (eds.), Elsevier Science, 1997.
[18] A. Bernasconi, M. Filippini, S. Foletti, D. Vaudo, Multiaxial fatigue of a railwheel steel under non-proportional loading. International Journal of Fatigue, 28 (2006), 663–672.
[19] M. Ciavarella, F. Monno, G. Demelio. On the Dang Van fatigue limit in rolling contact fatigue. International Journal of Fatigue, 28 (2006), 852–863.
[20] H. Desimone, A. Bernasconi, S. Beretta, On the application of Dang Van criterion to rolling contact fatigue. Wear 260 (2006), 568–571.
[21] S. Suresh, Fatigue of materials, Cambridge University Press, New York, 2006.
[22] R.B. Heywood, Designining against fatigue, Chapman and Hall Ltd., London, 1962.
[23] T.J. Dalan, in: O.J. Horger (Ed.), ASME Handbook, Metal Engineering Design, New York.
[24] J. Lai, T. Lund, K. Rydén, A. Gabelli, I. Strandell, The fatigue limit of bearing steels – Part I: A pragmatic approach to predict very high cycle fatigue strength. Int. Journal of Fatigue 37 (2012), 166–167.
[25] Y. Murakami, Metal Fatigue: Effects of Small defects and Nonmetallic Inclusions, Elsevier, Oxford, 2002.
[26] B. Atzori, G. Meneghetti, L. Susmel, Material fatigue properties for assessing mechanical components weakened by notches and defects. Fatigue Eng Mater, 28 (2005), 83–97.
[27] M.L. Roessle, A. Fatemi, Strain-controlled fatigue properties of steels and some simple approximations. Int. Journal of Fatigue, 22 (2000), 495–511.
[28] E.C. Santos, K. Honda, H. Koike, J. Rozwadowska, Fatigue strength improvement of AISI 52100 bearing steel by induction heating and repeated quenching. Material Science, 47 (2011), No. 5, 677 –682.